Genome-wide analysis of lncRNAs in 3'-untranslated regions: *CR933609* acts as a decoy to protect the *INO80D* gene

CHUN-CHI CHANG[1,2*], TING-YUAN LIU[3*], YA-TING LEE[4], YU-CHIA CHEN[3], KUN-TU YEH[5],
CHIEN-CHIN LEE[4], YA-LING CHEN[2,6], PEI-CHIN LIN[1,7], YA-SIAN CHANG[8*],
WEN-LING CHAN[4,9*], TA-CHIH LIU[1,10*] and JAN-GOWTH CHANG[3,4,8,11*]

[1]Institute of Clinical Medicine, College of Medicine, Kaohsiung Medical University, Kaohsiung 807;
[2]Division of Chest Medicine, Department of Internal Medicine, Changhua Christian Hospital, Changhua 500;
[3]Center for Precision Medicine, [4]Epigenome Research Center, China Medical University Hospital, Taichung 404;
[5]Department of Pathology, [6]Department of Nursing, Changhua Christian Hospital, Changhua 500;
[7]Division of Hematology and Oncology, Department of Pediatrics, Kaohsiung Medical University Hospital,
Kaohsiung 807; [8]Department of Laboratory Medicine, China Medical University, Taichung 404;
[9]Department of Bioinformatics and Medical Engineering, Asia University, Taichung 413;
[10]Division of Hematology and Oncology, Department of Internal Medicine,
Kaohsiung Medical University Hospital, Kaohsiung 807; [11]College of Medicine,
China Medical University, Taichung 404, Taiwan, R.O.C.

Abstract. Long non-coding RNAs (lncRNAs) have various functions, including chromatin remodeling and the regulation of gene expression at the transcriptional and post-transcriptional levels. However, few lncRNAs have been investigated comprehensively, with the majority being uncharacterized. In the present study, a bioinformatics pipeline was established to identify novel lncRNA sequences similar to the 3'-untranslated regions (3'-UTRs) of protein-coding genes. These pairs of lncRNAs and coding genes contained the same microRNA (miRNA) target sites; the lncRNA *CR933609* matched the 3'-UTR of INO80 complex subunit D (*INO80D*) mRNA. The expression levels of *CR933609* and *INO80D* were significantly decreased in non-small cell lung cancer (NSCLC) and other cancer tissues. The expression levels of *CR933609* and *INO80D* were decreased in *CR933609*-knockdown NSCLC cells, but only expression levels of *INO80D* decreased in *INO80D* knockdown cells. It was shown that there are independent promoters in *CR933609* and *INO80D*. It was also found that the expression levels of *INO80D* were downregulated by endogenous miRNA-5096 in A549 cells, but not in *CR933609*-overexpressing A549 cells. Furthermore, the lncRNA *CR933609* acted as a decoy to protect *INO80D* from downregulation by miRNA-5096 in NSCLC cells. A protocol was established to identify novel lncRNAs in the 3'-UTR and the existence of novel lncRNAs was confirmed.

Correspondence to: Dr Jan-Gowth Chang, Epigenome Research Center, China Medical University Hospital, 2 Yuh-Der Road, Taichung 404, Taiwan, R.O.C.
E-mail: d6781@mail.cmuh.org.tw

Dr Ta-Chih Liu, Division of Hematology and Oncology, Department of Internal Medicine, Kaohsiung Medical University Hospital, 100 Shih-Chuan 1st Road, Kaohsiung 807, Taiwan, R.O.C.
E-mail: d730093@kmu.edu.tw

*Contributed equally

Abbreviations: ANXA5, annexin A5; CMTM4, CKLF-like MARVEL trans-membrane domain containing 4; DSB, double strand break; EIF3B, eukaryotic translation initiation factor 3, subunit B; EIF4G2, eukaryotic translation initiation factor 4γ, 2; *INO80D*, INO80 complex subunit D; NSCLC, non-small cell lung cancer; RT-qPCR, reverse transcription-quantitative polymerase chain reaction; TAP2, transporter 2, ATP-binding cassette, subfamily B (MDR/TAP); lncRNA, long non-coding RNA

Introduction

At least 90% of the human genome is actively transcribed into non-coding RNAs (ncRNAs), whereas <2% of genome sequences encode proteins (1). Over the last 10 years, one type of ncRNA, namely microRNA (miRNA), has been increasingly investigated. miRNAs are ~21-23 nucleotides in length and are derived from long hairpin precursors. miRNAs are associated with Argonaute proteins, which post-transcriptionally regulate target genes, usually by binding to partially complementary sequences in the 3'-untranslated region (3'-UTR) of their mRNAs (2). The dysregulation of this process has been implicated in various biological disorders and human diseases.

Another category of ncRNAs, long non-coding RNAs (lncRNAs), has attracted considerable attention. The analysis

of high-throughput RNA sequencing data has provided a robust platform for investigating transcriptomes and has led to the identification of a large number of lncRNAs (3). lncRNAs are defined as endogenous cellular RNA molecules >200 nucleotides in length, which resemble mRNAs but lack coding potential and show poor sequence conservation between species (4-6). Previous studies have indicated that lncRNAs function as signal, decoy, guide, or scaffold RNAs (7,8). However, the characteristics of lncRNAs require further investigation. For example, lncRNAs can guide *cis*- or *trans*-acting epigenetic-modifying complexes to distinct genomic loci and can control the formation and spread of heterochromatin domains, thereby activating or repressing transcriptional activity (8). Additionally, lncRNAs possibly function as adaptors that direct chromatin-remodeling complexes and transcription factors to specific chromatin loci. lncRNAs can also act as scaffolds that recruit multiple proteins simultaneously to coordinate their activities (9). Studies have shown that the aberrant expression of lncRNAs including *BC200* (10,11), *H19* (12-16), *MALAT1* (17-20), *UCA1/CUDR* (21-23), *HOTAIR* (24-26) and *GAS6-AS1* (27) can cause various types of human cancer. These lncRNAs modulate gene transcription and translation, and RNA processing and chromatin remodeling, and have considerable potential as biomarkers, targets and therapeutic agents (5).

One particular human pseudogene, *PTENP1*, has been reported to regulate its corresponding protein-coding mRNA, transcribed from the phosphatase and tensin homolog gene, by acting as a decoy for miRNAs that bind to similar sequences in their respective 3'-UTRs (28). Furthermore, our previous study showed that the human pseudogene *ψPPM1K* may generate endogenous small interfering (si)RNA to suppress oncogenic cell growth in hepatocellular carcinoma (29). These studies prompted the hypothesis that there are further lncRNAs that require identification. Consequently, the present study performed a genome-wide bioinformatics screen and subsequent biological validation experiments to test this hypothesis.

Materials and methods

Bioinformatics. A flowchart for identifying lncRNAs that potentially act as miRNA decoys is shown in Fig. 1. Over 20,000 human lncRNA transcripts were obtained from NONCODE v.4 (30). The sequences of miRNAs and 3'-UTRs of protein-coding genes were collected from miRBase 20 (31) and UCSC hg19 (32), respectively. Previous approaches were modified to assess whether lncRNAs behave as miRNA decoys (29). Briefly, the sequences of lncRNAs and 3'-UTRs of protein-coding genes were aligned, and those lncRNAs (the same orientation as coding genes) showing >90% identity, termed 3'-UTR-like lncRNAs, were collected. These sequences were then analyzed using miRNA target prediction tools, miRTar-Base 6.0 (33,34), TargetScan 7.0 (35-37), miRanda 3.3a (38), and RNAhybrid 2.1.2 (20). The miRNA was selected according to the score of four databases and the binding energy. The 3'-UTR-like lncRNAs were all transcribed in the same direction as their corresponding coding genes and thus had the potential to act as miRNA decoys through reversed expression between lncRNA and its corresponding coding gene. The expression profiles of these lncRNA/coding-gene pairs in 460 squamous

cell carcinomas were obtained from The Cancer Genome Atlas (http://cancergenome.nih.gov/). To identify the functions of these corresponding coding genes, the Database for Annotation, Visualization and Integrated Discovery (DAVID) (39) annotation tool was used to assign Gene Ontology (GO) terms and to perform pathway analysis and promoter analysis.

Clinical specimens. Resected primary tumor and adjacent non-tumor tissue samples were obtained from 83 patients with NSCLC, 30 patients with kidney cancer, 30 patients with colon cancer, 30 patients with oral cancer, and 30 patients with liver cancer at either China Medical University Hospital (Taichung, Taiwan; CMUH) or Changhua Christian Hospital (Changhua, Taiwan; CCH). The tumor tissues were composed of 90-100% cancer cells. They were frozen immediately following surgical resection and then stored in liquid nitrogen until extraction of either RNA or DNA. All participants provided their written informed consent to participate in the study. The institutional review boards of CMUH and CCH approved the study (CMUH102-RECJ-015 and CCH-IRB-080322) and the consent procedure. The baseline characteristics of the NSCLC population in the present study are summarized in Table I.

Reverse transcription-quantitative polymerase chain reaction (RT-qPCR) analysis. Total RNA was extracted using the REzol reagent (Protech Technology Enterprise Co., Ltd., Taipei, Taiwan) according to the manufacturer's protocol and treated with RQ1 RNase-Free DNase (Promega Corporation, Madison, WI, USA). cDNA was generated from total RNA using the High-Capacity cDNA Reverse Transcription kit (Applied Biosystems; Thermo Fisher Scientific, Inc., Waltham, MA, USA). The RT-qPCR analysis was performed in a total reaction volume of 10 μl, including 1 μl of cDNA, 5 μl of LightCycler FastStart DNA Master HybProbe (Roche Diagnostics, Indianapolis, IN, USA), 0.6 μl of mixed primers (Table II), 1.2 μl of universal probes (Table II) (Roche Diagnostics), and 2.2 μl of double-distilled water. A LightCycler 480 (Roche Diagnostics) was used with the following program: Preincubation for 10 min at 95˚C; followed by 50 cycles of 10 sec at 95˚C, 30 sec at 60˚C, and 1 sec at 72˚C; and finally cooling to 4˚C. Glyceraldehyde-3-phosphate dehydrogenase (*GAPDH*) served as an internal reference. The relative RNA levels were calculated using the comparative quantification cycle method (39). The RT-qPCR product was verified through Sanger sequencing to ensure the primers specificity. Different target sites were verified to ensure primer specificity. INO80 Complex Subunit D (INO80D): Primer target on exon 5-exon 6 (ΔCq, 9.92±0.33), primer target on exon 11 used in the present study (ΔCq, 9.45±0.36), primer target on exon 11 (ΔCq, 9.41±0.27). CR933609: primer used in the present study (ΔCq, 7.38±0.16), primer target on other site (ΔCq, 7.86±0.61).

Northern blots. Total RNA was extracted from cells by using REzol C&T RNA extraction reagent (Protech Technology Enterprise Co., Ltd.). Following extraction, 15 μg of total RNA was dissolved in a loading buffer containing 10 mM EDTA (pH 8.0), 96% (v/v) formamide, 0.01% xylene cyanol, and 0.01% bromophenol blue, heated at 95˚C for 5 min, loaded onto a 1% MOPS 3-(N-morpholino) propanesulfonic acid gel with 2% formamide, separated for 2 h at 150 V, and then transferred
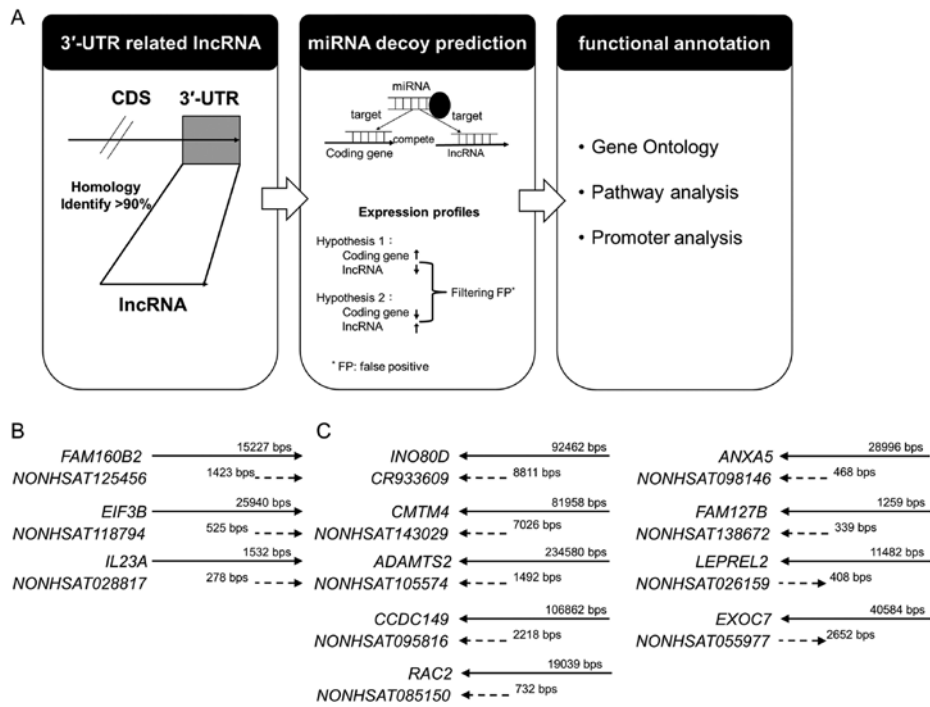
Figure 1. Flowchart for the identification of lncRNAs that potentially act as miRNA decoys. (A) A set of 3'-UTR-related lncRNAs were identified by surveying the genome for sequence matches between the 3'-UTRs of protein-coding genes and lncRNAs. Subsequently, miRNA target sites in these matching regions were predicted using four miRNA target prediction tools. To determine that an lncRNA acts as an miRNA decoy, the reversed expression profiles of the lncRNA and its paired coding genes were collected. Finally, Gene Ontology, pathway analysis, and promoter analysis were applied to examine the functional annotation. Mapping results for 12 human lncRNA transcripts showing high matches with 3'-UTRs of protein-coding genes are shown. Most of these 12 lncRNAs were transcribed in the same direction as their corresponding genes and thus have a potential role as miRNA decoys. (B) Sense transcriptions of lncRNAs and their corresponding genes. (C) Antisense transcriptions of lncRNAs and their corresponding genes. lncRNAs, long non-coding RNAs; 3'-UTR, 3'-untranslated region; miRNA microRNA.

Table I. Clinical variables and relative gene expression of the long non-coding RNA *CR933609* in non-small cell lung cancer.

Characteristic	CR933609			INO80D		
	n	ΔCq[a]	P-value	n	ΔCq[a]	P-value
Age (years)						
<65	33	5.35±1.56	0.469	33	5.91±1.31	0.129
≥65	50	5.07±1.73		50	5.38±1.65	
Sex						
Men	48	5.43±1.79	0.105	48	5.68±1.52	0.554
Women	35	4.84±1.42		35	5.47±1.56	
Smoking						
Never	46	4.96±1.45	0.197	46	5.51±1.59	0.607
Current/ex-smoker	37	5.45±1.87		37	5.69±1.48	
ECOG PS						
0	38	4.99±1.50	0.336	38	5.36±1.59	0.213
1	45	5.34±1.78		45	5.78±1.48	
Histology						
Adenocarcinoma	51	4.66±1.37	0.001	51	5.40±1.42	0.165
Squamous cell carcinoma	32	6.01±1.77		32	5.89±1.68	
Grade						
Well/moderate	72	5.19±1.66	0.925	72	5.53±1.58	0.351
Poor differentiation	11	5.14±1.73		11	5.99±1.18	
Stage						
I+II	65	5.19±1.67	0.973	65	5.51±1.59	0.350
III+IV	18	5.17±1.67		18	5.89±1.31	

[a]Data shown as mean ± standard deviation. ECOG PS, Eastern Cooperative Oncology Group Performance Status; *INO80D*, INO80 complex subunit D.

Table II. Primer sequences.

Name	Forward primer (5'-3')	Reverse primer (5'-3')	Probe no.
NONHSAT143029	ggccaggtctgggagataag	atagcagacaggtggggtgt	38
CMTM4	tgcggcatatgcagtgaa	gctcggatgtagtcattggtg	72
NONHSAT095816	cctgcaaatgtccagcacta	aaacttggctgtgtttttccttc	21
CCDC149	ctcacctggactccttcgag	atccctttgccgtcttcc	66
NONHSAT085150	ccaatggaaaatctgggttc	caggtaagtgcagctcagga	84
RAC2	cccagcctcttatgagaacg	gtgcccaccaggatgatg	43
NONHSAT026159	accccaccatcctcttcatt	aacactgtgcctccctgaac	75
LEPREL2	cagggtgctaagctgcttct	caggtgggtgaaggacagat	7
NONHSAT118794	gcggttcctctgttgcag	cagagccagagagcacagg	4
EIF3B	ggtggacactgacgagctg	gacgaagaactcaatggtctcc	48
NONHSAT105574	tggaagcctttgggaagag	cttcagcggaagacaggtg	33
ADAMTS2	cctatgactgcctgctggat	attgctcgttcatggagtagtg	43
NONHSAT028817	gctgacctatgataaggttgagtattt	caataaataatcctccccaaactg	79
IL23A	cttctccgcttcaaaatcctt	tgctccatgggcaaagac	5
NONHSAT138672	ctggcaaccaaatcgaatct	aaaggcacccatcagagaga	2
FAM127B	gaaggtgacgttcctcatcac	cccggtaatcattgagcag	12
NONHSAT055977	caccatgtcctcctcccta	ggtcacctgggacttcagg	43
EXOC7	tgcacaagcagacggaga	gcaggacagcgtcttctca	2
NONHSAT098146	aagagctccctgctgtgtg	tggcatacaaatgcagctaaag	8
ANXA5	tctgtttggcagggatcttc	tcataaagccgagagggtttc	21
NONHSAT125456	gagcagtgaatgggatcgtc	ctgggagttttgcaacagttt	4
FAM160B2	aggactgctcccacgatg	agctcctcggtctcagca	5
CR933609	gacaaaacaaactagtgaagcacct	tatacaccttgacacggcaga	47
INO80D	cctgatgacttacaagattttgattt	ctcctcagcctcttcggtag	52
GAPDH	agccacatcgctcagacac	gcccaatacgaccaaatcc	60

Probe numbers were obtained from Universal Probe Library (Roche Diagnostics, Indianapolis, IN, USA).

onto nitrocellulose membranes (Pall Corporation, East Hills, NY, USA). The subsequently underwent cross-linking with UV irradiation for 5 min. The membranes with RNA blots were prehybridized at 42°C for 3 h using digoxigenin (DIG) Easy Hyb Granules (Roche Diagnostics) and subjected to hybridization with a DIG probe for the lncRNA *NONHSAT098146* (0.1 μg/ml) overnight at 42°C. Following hybridization, the membranes were rinsed and then washed sequentially with 2X SSC/0.1% sodium dodecyl sulfate (SDS) and 0.1X SSC/0.1% SDS at 42°C. Detection was performed using the DIG Northern Starter kit (Roche Diagnostics) according to the manufacturer's protocol. The blots were detected with a chemiluminescent substrate (CDP-Star) and visualized using the ChemiDoc-It imaging system (UVP, Inc., Upland, CA, USA).

Cell culture, and siRNA and short hairpin (sh)RNA transfection. Cells from the A549, H441, and H520 NSCLC lines [Bioresource Collection and Research Center (BCRC), Hsinchu, Taiwan] were cultured in Dulbecco's modified Eagle's medium (DMEM; Gibco; Thermo Fisher Scientific,) supplented with 10% fetal bovine serum (FBS; Gibco; Thermo Fisher Scientific, Inc.) at 37°C in a 5% CO_2 atmosphere. The oligonucleotides used for three siRNA and *INO80D*/annexin A5 (*ANXA5*) shRNA constructs are shown in Table III. The *INO80D* and

ANXA5 shRNAs were obtained from the National Research Program for Biopharmaceuticals (Taipei, Taiwan). The A549 cells were transfected with the shRNAs (6 μg of *INO80D* shRNA in 2x10 A549 cells/ml) using Lipofectamine 2000 (Thermo Fisher Scientific, Inc.). The efficiency of transfection was determined using RT-qPCR analysis.

Establishment of CR933609-overexpressing and NONHSAT098146-overexpressing stable cell lines. The cDNA from the lncRNAs *CR933609* and *NONHSAT098146* was cloned in pCDNA3.0 (Invitrogen; Thermo Fisher Scientific, Inc.). The A549 cells ($2x10^6$) were transfected with *CR933609*-overexpressing, *NONHSAT098146*-overexpressing, and control vectors using Lipofectamine 2000 (Thermo Fisher Scientific, Inc.). Following 48 h of recovery, the transfected cells were cultured in a medium containing 500 μg/ml G418 for 2-3 weeks. Clones representing stable cell lines were then selected and expanded to large-scale cultures. The RNA extracts prepared from these clones were analyzed for target RNA levels using RT-qPCR analysis.

Cell proliferation assay. To examine whether lncRNA knockdown altered the viability of NSCLC cells, cell proliferation assays were performed. Briefly, 10,000 cells from the NSCLC

Table III. Oligonucleotides for siRNA and shRNA constructs.

Symbol	Ref ID	Target sequence (5'-3')	Note
siRNA1	FR273090	GGGCACGTGTGTGAGAGATATGAAT	Common region with *CR933609* and *INO80D*
siRNA2	FR273090	CAGACATGAGCTGTGTTTATCTATT	Common region with *CR933609* and *INO80D*
siRNA3	FR273090	GGGATCATTTCACCGTGCATATTTC	Common region with *CR933609* and *INO80D*
shRNA1	NM_017759	GCACTTACTTTCAGCAGAAAT	*INO80D*-specific
shRNA2	NM_017759	CCATTTGCTTTCAATGAGGAA	*INO80D*-specific
shRNA3	NM_017759	CAACATCGTACTCTGGTGATA	*INO80D*-specific
shRNA4	NM_017759	CTATTGAATGGGCGTATAGTA	*INO80D*-specific
shRNA5	NM_017759	GAGCTATTGAATGGGCGTATA	*INO80D*-specific
NONHSAT098146	NONHSAT098146	GUGUACUUAAUGUUACUAAdTdT	Common region with *NONHSAT098146* and *ANXA5*
ANXA5-homo-531	NM_001154	GAGCCAUCAAACAAGUUUATT	*ANXA5*-specific
ANXA5-homo-993	NM_001154	GUGAGAUUGAUCUGUUUAATT	*ANXA5*-specific
ANXA5-homo-844	NM_001154	CGAGACUUCUGGCAAUUUATT	*ANXA5*-specific

siRNA, small interfering RNA; shRNA, short hairpin RNA; *INO80D*, INO80 complex subunit D; *ANXA5*, annexin A5.

cell lines, stable transfectants subjected to lncRNA knockdown or parental NSCLC cell lines, were cultured in DMEM with 10% FBS (according to the BCRC). After 72 h, cell proliferation and viability were assessed using the 3-(4,5-dimethylthiazol-2-yl)-2,5-diphenyl-tetrazolium bromide assay. All experiments were performed in triplicate.

Wound-healing assay. A wound-healing assay was conducted to assess cell migration. The basic steps involved creating a 'wound' in a cell monolayer, capturing images at the beginning and at regular intervals as cells migrated into the wound, and comparing the images to quantify the cell migration rate. For each assay, 2×10^5 cells were plated in 48-well plates (Corning Costar, Schiphol-Rijk, The Netherlands) with serum-free medium. A 200-μl plastic pipette tip was drawn across the center of the well to produce a clean wound of ~1 mm in width in the cell monolayer.

miRNA-mediated knockdown of CR933609 and INO80D. A stable negative control (siCon: 5'-FAM-UUCUCCGAACGU GUCACGUTT-3') and has-miR-5096 were purchased from GeneDireX, Inc. (Las Vegas, NV, USA) and transfected into cells using Lipofectamine RNAiMax (Invitrogen; Thermo Fisher Scientific, Inc.) according to the manufacturer's protocol. The efficacy of mRNA knockdown following miRNA transfection for 48 h was determined using RT-qPCR analysis.

Luciferase reporter assay. Fragments of DNA from the lncRNA *CR933609* promoter region were obtained through PCR amplification and cloned into the pGL3-basic reporter vector (Promega Corporation). The constructs were transfected into A549 cells (2×10^6) using Lipofectamine 2000 (Thermo Fisher Scientific, Inc.). The cells were lysed and assayed for luciferase activity using the Steady-Glo Luciferase

assay system (Promega Corporation) according to the manufacturer's protocol at 24 h post-transfection.

Statistical analysis. All data are presented as the mean ± standard deviation or as percentages. Statistical analyses, including the χ^2 test, independent t-test, one-way analysis of variance followed by Fisher's least significant difference post hoc test, and paired t-test, were performed using SPSS version 17.0 software (SPSS, Inc., Chicago, IL, USA. $P < 0.05$ was considered to indicate a statistically significant difference.

Results

Overview of lncRNAs. The bioinformatics analysis (Fig. 1A) showed that 12 human lncRNA transcripts contained sequences with significant matches to the 3'-UTRs of protein-coding genes (Table IV). These lncRNAs were all transcribed in the same direction as their corresponding coding genes and thus have the potential to act as miRNA decoys (Fig. 1B and C). To identify the functions of these protein-coding genes, the annotation tool DAVID (40) was used to assign GO terms. Certain GO biological process terms that were significantly associated with the coding genes, including regulation of translational initiation [eukaryotic translation initiation factor (*EIF*)*4G2* and *EIF3B*; $P < 0.03$] and response to chemical stimulus [ras-related C3 botulinum toxin substrate 2, transporter 2, ATP-binding cassette, subfamily B (*TAP2*), RNA binding motif protein 4, *ANXA5* and CKLF-like MARVEL trans-membrane domain containing 4 (*CMTM4*); $P < 0.03$], and molecular-function terms, including receptor binding [interleukin 23 α subunit p19 (*IL23A*), *TAP2*, relaxin 2, *ANXA5* and *CMTM4*; $P < 0.01$] (data not shown).

Expression profiles of lncRNAs and parental coding genes in NSCLC. The average (Fig. 2) expression levels of lncRNAs and

Table IV. Basic data of 12 human lncRNA transcripts with high homology with 3'-UTRs of protein-coding genes.

No.	Transcript ID	Type	Chromosome	Start site	End site	Strand	Exon	Length	3'-UTR similarity	ncRNA similarity
1	*CR933609*	lncRNA	2	206,858,445	206,867,214	-	1	8,811	0.99	1
	INO80D	Gene	2	206,858,445	206,950,906	-	11	92,462		
2	*NONHSAT143029*	lncRNA	16	66,648,652	66,655,678	-	1	7,026	0.96	1
	CMTM4	Gene	16	66,648,653	66,730,610	-	5	81,958		
3	*NONHSAT105574*	ncRNA	5	178,537,853	178,540,736	-	1	1,492	0.96	1
	ADAMTS2	Gene	5	178,537,852	178,772,431	-	22	234,580		
4	*NONHSAT095816*	lncRNA	4	24,807,739	24,809,957	-	1	2,218	0.98	1
	CCDC149	Gene	4	24,807,739	24,981,826	-	13	106,862		
5	*NONHSAT125456*	lncRNA	8	21,960,467	21,961,890	+	1	1,423	0.98	1
	FAM160B2	Gene	8	21,958,951	21,961,891	+	4	15,227		
6	*NONHSAT085150*	lncRNA	22	37,621,303	37,622,035	-	1	732	0.94	1
	RAC2	Gene	22	37,621,310	37,640,305	-	7	19,039		
7	*NONHSAT118794*	lncRNA	7	2,419,855	2,420,380	+	1	525	0.94	0.99
	EIF3B	Gene	7	2,394,474	2,420,377	+	19	25,940		
8	*NONHSAT098146*	lncRNA	4	122,589,152	122,589,620	-	1	468	0.99	1
	ANXA5	Gene	4	122,589,152	122,618,147	-	13	28,996		
9	*NONHSAT138672*	lncRNA	X	134,184,962	134,185,301	-	1	339	0.9	1
	FAM127B	Gene	X	134,184,963	134,186,221	-	2	1,259		
10	*NONHSAT028817*	lncRNA	12	56,733,915	56,734,193	+	1	278	0.91	1
	IL23A	Gene	12	56,732,663	56,734,194	+	4	1,532		
11	*NONHSAT026159*	lncRNA	12	6,948,604	6,949,010	+	1	408	0.99	1
	LEPREL2	Gene	12	6,937,538	6,949,018	-	5	11,482		
12	*NONHSAT055977*	lncRNA	17	74,097,193	74,099,845	+	1	2,652	0.99	1
	EXOC7	Gene	17	74,077,086	74,099,868	-	20	40,584		

3'-UTR, 3'-untranslated region; lncRNA, long non-coding RNA.

parental genes were quantitatively analyzed through RT-qPCR analysis. The results showed that the expression levels of lncRNAs and parental genes were lower in cancer tissues than in non-tumor tissues. These results were summarized from observations at either CMUH or CCH. The expression levels of lncRNAs in a small number of samples were undetectable, which is the reason for the difference in the number of samples. The expression levels of *INO80D* and the 3'-UTR-like lncRNA *CR933609* were significantly lower in the cancerous tissues (P<0.01). The expression levels of *ANXA5* and the 3'-UTR-like lncRNA *NONHSAT098146* showed the most marked change. *INO80D* is involved in the transcription-coupled nucleotide excision repair and DNA double-strand break (DSB) repair pathways. In addition, DNA DSBs contribute to the genomic instability driving cancer development. Therefore, *INO80D* and *CR933609* were selected for the subsequent investigations. The *INO80D* and the 3'-UTR-like lncRNA *CR933609* pair, and the *ANXA5* and the 3'-UTR-like lncRNA *NONHSAT098146* pair were selected for further examination.

Association between lncRNAs and parental coding genes. INO80 Complex Subunit D (*INO80D*), a protein-coding gene located on chromosome 2q33.3, is involved in transcriptional regulation and possibly DNA repair (41). The computational

results showed that the sequence of the lncRNA *CR933609*, which maps to the same region of chromosome 2, is 99% identical to the region of 8,762 nucleotides in the 3'-UTR of *INO80D* (Fig. 3A, top). This result suggested that the *CR933609* transcriptional unit is embedded in the *INO80D* gene.

ANXA5, a protein-coding gene located on chromosome 4q27, is implicated in membrane-related events along exocytotic and endocytotic pathways (42). The computational results showed that the sequence of the lncRNA *NONHSAT098146*, which maps to the same region of chromosome 4, is 100% identical to the region of 468 nucleotides in the 3'-UTR of *ANXA5* (Fig. 3B, top). This result suggested that the *NONHSAT098146* transcriptional unit is embedded in the *ANXA5* gene.

To examine whether *CR933609* and *NONHSAT098146* act as miRNA decoys, and thereby modulate miRNA regulation in *INO80D* and *ANXA5*, four miRNA target prediction tools were used to investigate possible target sequences within the *INO80D* and *CR933609* transcripts and the *ANXA5* and *NONHSAT098146* transcripts. The results indicated that miRNA-5096 interacts with a sequence within the common regions of *CR933609* and *INO80D* (Fig. 3A, bottom), and miRNA-4694-3p potentially interacts with a sequence within the common regions of *NONHSAT098146* and *ANXA5* (Fig. 3B, bottom). The microRNA, hsa-mir-5096, was selected
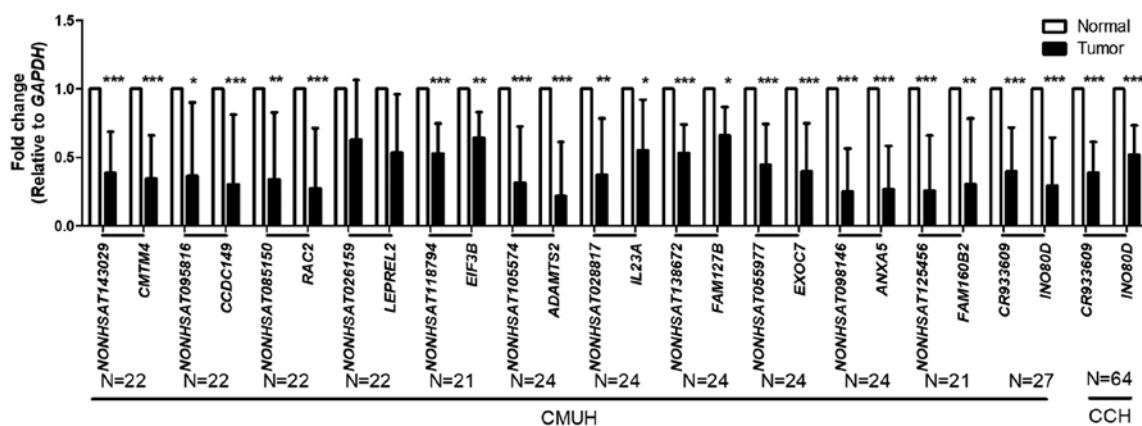
Figure 2. Expression levels of lncRNAs and parental genes in non-small cell lung cancer. The expression levels of lncRNAs and parental genes were quantitatively analyzed using reverse transcription-quantitative polymerase chain reaction analysis. The internal control was *GAPDH*. The white bar denotes the normal region, and the black bar denotes the tumor region. Error bars represent the standard deviation. Student's t-test was performed to evaluate differences between the groups. *$P<0.05$, **$P<0.01$ and ***$P<0.001$, compared with normal region. The results are summarized from observations at either CMUH or CCH. lncRNAs, long non-coding RNAs; *GAPDH*, glyceraldehyde-3-phosphate dehydrogenase; CMUH, China Medical University Hospital; CCH, Changhua Christian Hospital.

Figure 3. Associations between *INO80D* and *CR933609*, and between *ANXA5* and *NONHSAT098146*. (A) *INO80D* is a protein-coding gene located on chromosome 2q33.3. Computational results showed that the lncRNA *CR933609* matches the 3'-UTR of *INO80D* with 99% identity. To examine whether *CR933609* acts as an miRNA decoy, four miRNA target prediction tools were used to investigate potential miRNA interactions with *INO80D* and *CR933609*. miRNA-5096 was found to be a likely candidate for interaction with the common regions of *CR933609* and *INO80D*. (B) *ANXA5*, a protein-coding gene located on chromosome 4q27, is implicated in membrane-related events along exocytotic and endocytotic pathways. The computational results showed that the sequence of the lncRNA *NONHSAT098146*, which maps to the same region of chromosome 4, was 100% identical to a 468-nucleotide region in the 3'-UTR of *ANXA5*. To ascertain whether *NONHSAT098146* acts as an miRNA decoy, four miRNA target prediction tools were used to investigate potential miRNA interactions with *ANXA5* and *NONHSAT098146*. miRNA-4694-3p was found to be a likely candidate for interaction with the common regions of *ANXA5* and *NONHSAT098146*. miRNA/miR, microRNA; lncRNA, long non-coding RNA; *INO80D*, INO80 complex subunit D; *ANXA5*, annexin A5.

as a candidate according to the score of four databases and the lowest binding energy (-16.34 kCal/mol), and so was miRNA-4694-3p (-34.49 kCal/mol).

Expression levels of selected lncRNAs and parental coding genes in five types of solid tumor. To determine the expression levels of the selected lncRNAs and parental genes in cancer, RT-qPCR analysis was used to measure the mRNA expression levels of *CR933609* and *INO80D* in five types of solid tumor. The *CR933609* and *INO80D* pair had significantly lower mRNA expression levels in the tumors of lung, colon and kidney cancer, compared with their adjacent non-tumor tissues (Fig. 4A). The *NONHSAT098146* and *ANXA5* pair exhibited significantly lower mRNA expression levels in the tumors of lung, colon, and kidney cancer, compared with their adjacent non-tumor tissues (Fig. 4B). Notably, the *NONHSAT098146* and

ANXA5 pair had significantly higher mRNA expression levels in mucosal tumors. It was also found that, in individual tumors and in A549 NSCLC cells, the expression levels of *CR933609* were higher than the expression levels of *INO80D* (Fig. 4C). However, the expression levels of *NONHSAT098146* were lower than the expression levels of *ANXA5* (Fig. 4D). As lung cancer is the leading cause of cancer-associated mortality worldwide, with NSCLC being the most prominent subgroup accounting for >80% of all lung cancer cases (43), the following experiments focused on NSCLC. Among types of NSCLC, the expression levels of *CR933609* were significantly lower in squamous cell carcinoma than in adenocarcinoma (P=0.001; Table I).

Associations between the expression of CR933609 and INO80D, and expression of NONHSAT098146 and ANXA5 in NSCLC cells. To examine the association between *CR933609*
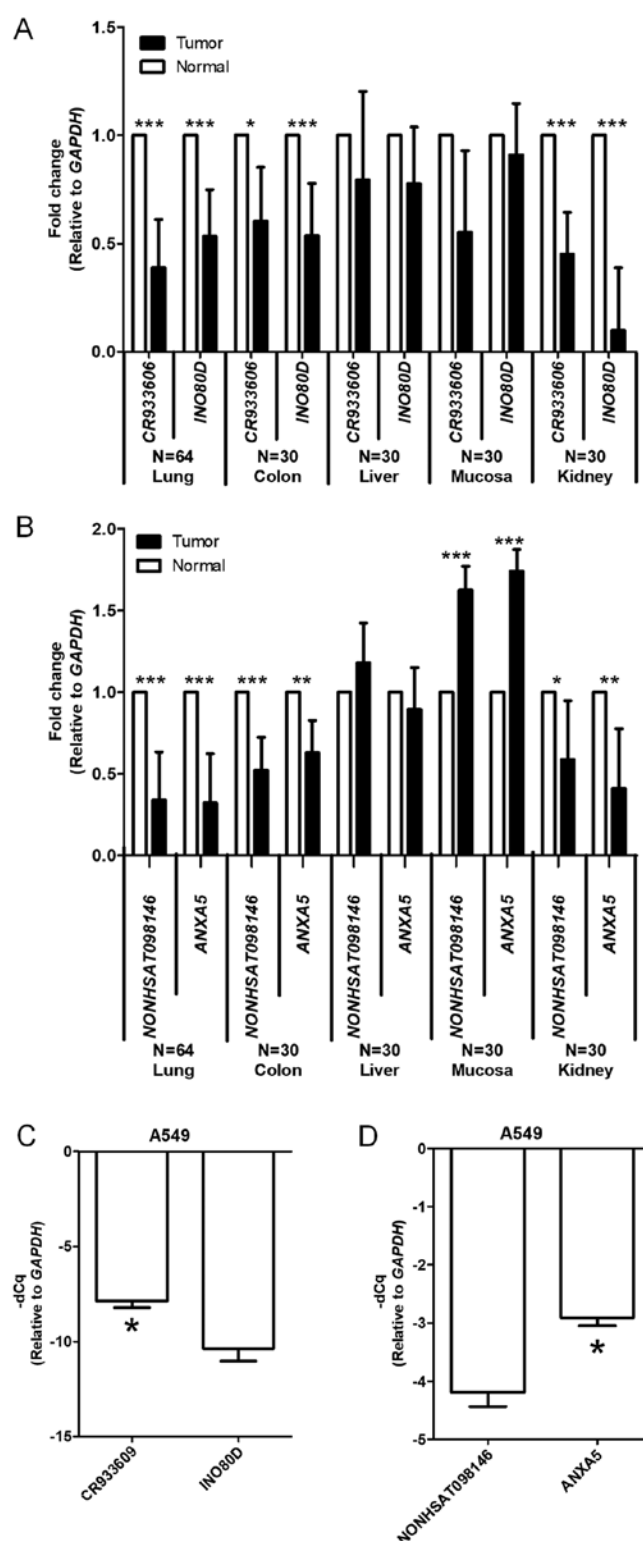
Figure 4. Gene expression levels of *CR933609* and *INO80D*, and *NONHSAT098146* and *ANXA5* are similar between various solid tumors and A549 cells. (A) Expression levels of *CR933609* and *INO80D* genes were quantitatively analyzed by using RT-qPCR analysis. The internal control was *GAPDH*. The white bar denotes the normal region, the black bar denotes the tumor region. Error bars represent the standard deviation. Student's t-test was used to evaluate differences between the groups. *P<0.05 and ***P<0.001, compared with normal region. The results are summarized from observations at CMUH. (B) Gene expression levels of *NONHSAT098146* and *ANXA5* were quantitatively analyzed using RT-qPCR analysis. The internal control was *GAPDH*. The white bar denotes the normal region and the black bar denotes the tumor region. Error bars represent the standard deviation. Student's t-test was used to evaluate differences between the groups. *P<0.05, **P<0.01 and ***P<0.001, compared with normal region. Results are summarized from observations at CMUH. (C) Expression levels of *CR933609* and *INO80D* genes were quantitatively analyzed using RT-qPCR analysis. The internal control was *GAPDH*. Error bars represent the standard deviation. Student's t-test was used to evaluate differences between the groups. *P<0.05, compared with the *INO80D* group. The results are summarized from observations of three independent experiments. (D) Gene expression levels of *NONHSAT098146* and *ANXA5* were quantitatively analyzed using RT-qPCR analysis. The internal control was *GAPDH*. Error bars represent the standard deviation. Student's t-test was used to evaluate differences between the groups. *P<0.05, compared with the *ANXA5* group. The results are summarized from observations of three independent experiments. RT-qPCR, reverse transcription-quantitative polymerase chain reaction analysis; *INO80D*, INO80 complex subunit D; *ANXA5*, annexin A5; *GAPDH*, glyceraldehyde-3-phosphate dehydrogenase; CMUH, China Medical University Hospital; CCH, Changhua Christian Hospital.
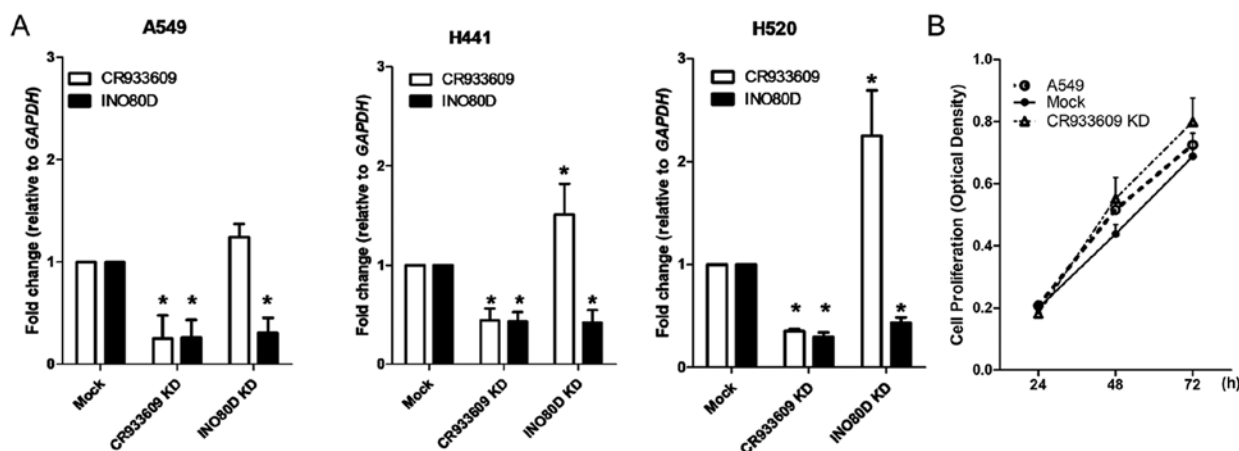
Figure 5. Expression levels of *CR933609* and *INO80D* decrease in *CR933609*-KD NSCLC cells but not in *INO80D*-KD cells. (A) Total RNA was isolated and subjected to reverse transcription-quantitative polymerase chain reaction analysis to detect RNA expression levels of *CR933609* (white) and *INO80D* (black) in NSCLC cells. The fold change was standardized using mRNA expression levels of *GAPDH*, relative to the mock group. (B) Cell proliferation was detected using the MTT assay between 24 and 72 h. The optical density of the experiment was standardized using the optical density of empty wells. Error bars represent the standard deviation. A Student's t-test was used to evaluate differences between the groups. *P<0.05, compared with the mock group. The results are summarized from observations of three independent experiments. NSCLC, non-small cell lung cancer; *INO80D*, INO80 complex subunit D; *GAPDH*, glyceraldehyde-3-phosphate dehydrogenase; KD, knockdown.

Figure 6. lncRNA CR933609 has different promoters to the *INO80D* gene. (A) Activity of promoters determined using a luciferase assay upstream of *CR933609*. The human cytomegalovirus promoter was a positive control. Mock cells were transfected with luciferase only. Error bars represent the standard deviation. Student's t-test was used to evaluate differences with respect to the mock group. *P<0.05, compared with the mock group. The results are summarized from observations of three independent experiments. (B) Diagram showing the location of the *CR933609* promoter. lncRNA, long non-coding RNA; UTR, untranslated region; *INO80D*, INO80 complex subunit D.

and *INO80D*, cells from three NSCLC lines, namely A549, H441 and H520 cells, were transfected with siRNAs (representing their common regions) and shRNAs (specifically targeted to *INO80D*). The siRNAs downregulated *CR933609* and *INO80D* in NSCLC cells (Fig. 5A), whereas the cell proliferation assay revealed that the siRNA-transfected cells showed
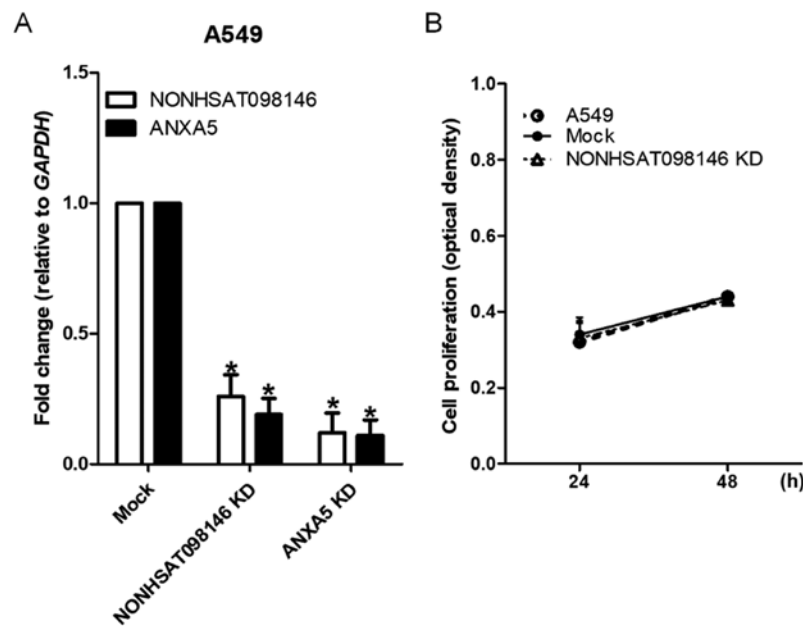
Figure 7. Expression levels of *NONHSAT098146* and *ANXA5* decrease in KD A549 cells. (A) Total RNA was isolated and subjected to reverse transcription-quantitative polymerase chain reaction analysis to detect RNA expression levels of *NONHSAT098146* (white) and *ANXA5* (black) in A549 cells. The fold change was standardized using mRNA expression levels of *GAPDH*, relative to the mock group. (B) Cell proliferation was detected using the MTT assay between 24 and 48 h. The optical density of the experiment was standardized using the optical density of empty wells. Error bars represent the standard deviation. Student's t-test was used to evaluate differences between the groups. *P<0.05, compared with the mock group. The results are summarized from observations of three independent experiments. *ANXA5*, annexin A5; *GAPDH*, glyceraldehyde-3-phosphate dehydrogenase; KD, knockdown.

a marginally higher proliferation rate, compared with that in the control (Fig. 5B). Notably, the downregulation of *INO80D* resulted in decreased expression levels only in *INO80D* (Fig. 5A). These results suggested that *CR933609* and *INO80D* have distinct transcripts. To determine whether *CR933609* and *INO80D* have different promoters, a luciferase reporter assay was used to identify the promoter of *CR933609*. As shown in Fig. 6A, a significant increase in luciferase activity was detected in constructs containing DNA fragments extending between -3602 and 0, -3602 and -3207, and -3602 and -3049 nucleotides upstream of the *CR933609* transcription initiation site, indicating a possible location of the *CR933609* promoter in the region between -3602 and -3360 nucleotides (Fig. 6B). Although the *CR933609* sequence is embedded within the *INO80D* gene, it is transcribed from a different promoter.

To examine the association between *NONHSAT098146* and *ANXA5*, the A549 cells were transfected with artificial siRNAs (representing their common regions) and shRNAs (specifically targeted to *ANXA5*). *NONHSAT098146* and *ANXA5* were underexpressed in *NONHSAT098146* knockdown and *ANXA5* knockdown cells, respectively (Fig. 7A). Cell proliferation was stable in the *NONHSAT098146*-knockdown cells (Fig. 7B). These results indicated that *NONHSAT098146* and *ANXA5* have the same transcripts. The RNA expression of the lncRNA *NONHSAT098146* was identified through northern blotting. The results showed that *NONHSAT098146* hybridization signals [468 base pairs (bp)] were invisible, whereas *ANXA5* hybridization signals (1,762 bp) were present in the cells (Fig. 8). Therefore, the lncRNA *NONHSAT098146* may be an artificial gene.

Established lncRNA-overexpressing stable cell lines. To examine the effect of the overexpression of lncRNA *CR933609*,
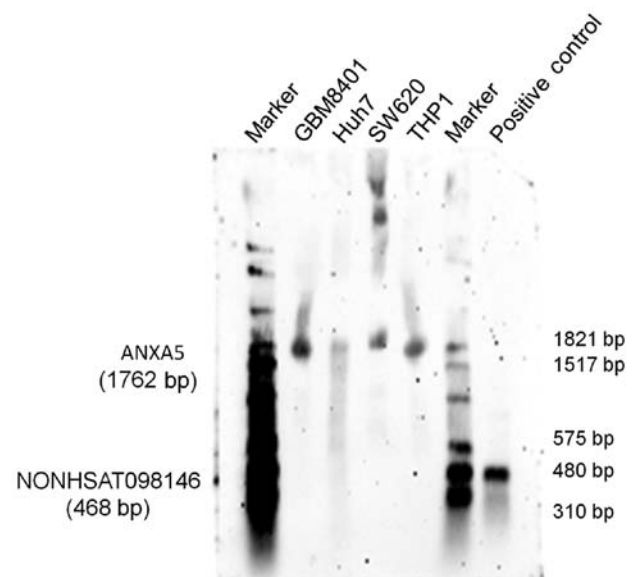

Figure 8. Long non-coding RNA *NONHSAT098146* cannot be detected through northern blotting. Northern blotting revealed that *NONHSAT098146* hybridization signals (468 bp) were not visible in the examined cell lines. *ANXA5* hybridization signals (1,762 bp) were present in the cell lines. The marker was DIG-labeled RNA with 40 µg (left) and 20 µg (right). The positive control was DIG-labeled *NONHSAT098146* RNA produced through *in vitro* transcription. The marker size is labeled on the right side. *ANXA5*, annexin A5.

the A549 cells were transfected with a *CR933609* recombinant plasmid vector, and stable and control clones were isolated. The gene expression of *CR933609* increased by >2.5-fold in the *CR933609*-overexpressing cells, compared the vector control cells, but no change in *INO80D* was observed (Fig. 9A). No
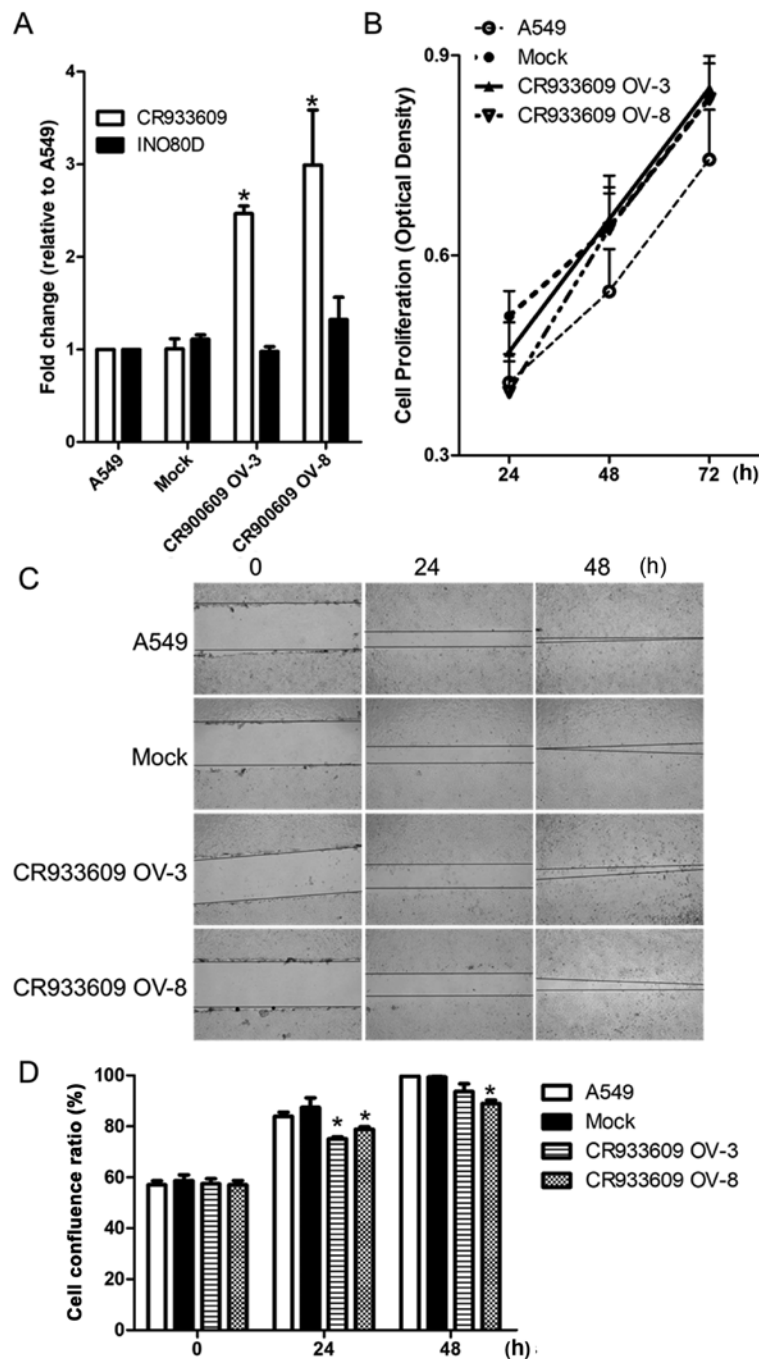
Figure 9. Established *CR933609*-overexpressing stable clone. (A) Total RNA was isolated and subjected to reverse transcription-quantitative polymerase chain reaction analysis to detect RNA expression levels of *CR933609* (white) and *INO80D* (black) in the A549 cell line and stable clone. The fold change was standardized using mRNA expression levels of glyceraldehyde-3-phosphate dehydrogenase, relative to A549. (B) Cell proliferation was detected using the MTT assay between 24 and 72 h. The optical density of the samples was standardized using the optical density of empty wells. (C) Wound-healing assay for A549 and stable clone. (D) Bar figure showing the quantitative results of the wound-healing assay. Error bars represent the standard deviation. Student's t-test was used to evaluate differences between groups. *P<0.05, compared with the A549 group or 0-h group. The results are summarized from observations of three independent experiments. *INO80D*, INO80 complex subunit D; OV, overexpression.

significant change in cell proliferation was observed in the *CR933609*-overexpressing cells (Fig. 9B). It was found that cell migration was significantly decreased in the *CR933609*-overexpressing cells (Fig. 9C and D). Therefore, *CR933609* may act as a tumor suppressor gene.

NONHSAT098146-overexpressing stable cell lines were established to ascertain the effect of overexpression. The expression of *NONHSAT098146* increased by 2-fold in *NONHSAT098146*-overexpressing cells, compared with the

vector control cells, but no change in *ANXA5* was observed (Fig. 10A). No significant differences in proliferation or migration were observed in the *NONHSAT098146*-overexpressing cells (Fig. 10B-D). These established cell lines were used in the subsequent experiment.

lncRNA CR933609 acts as a repressor decoy to prevent downregulation of expression levels of INO80D. As shown in Fig. 11A (top), the expression levels of *CR933609* and
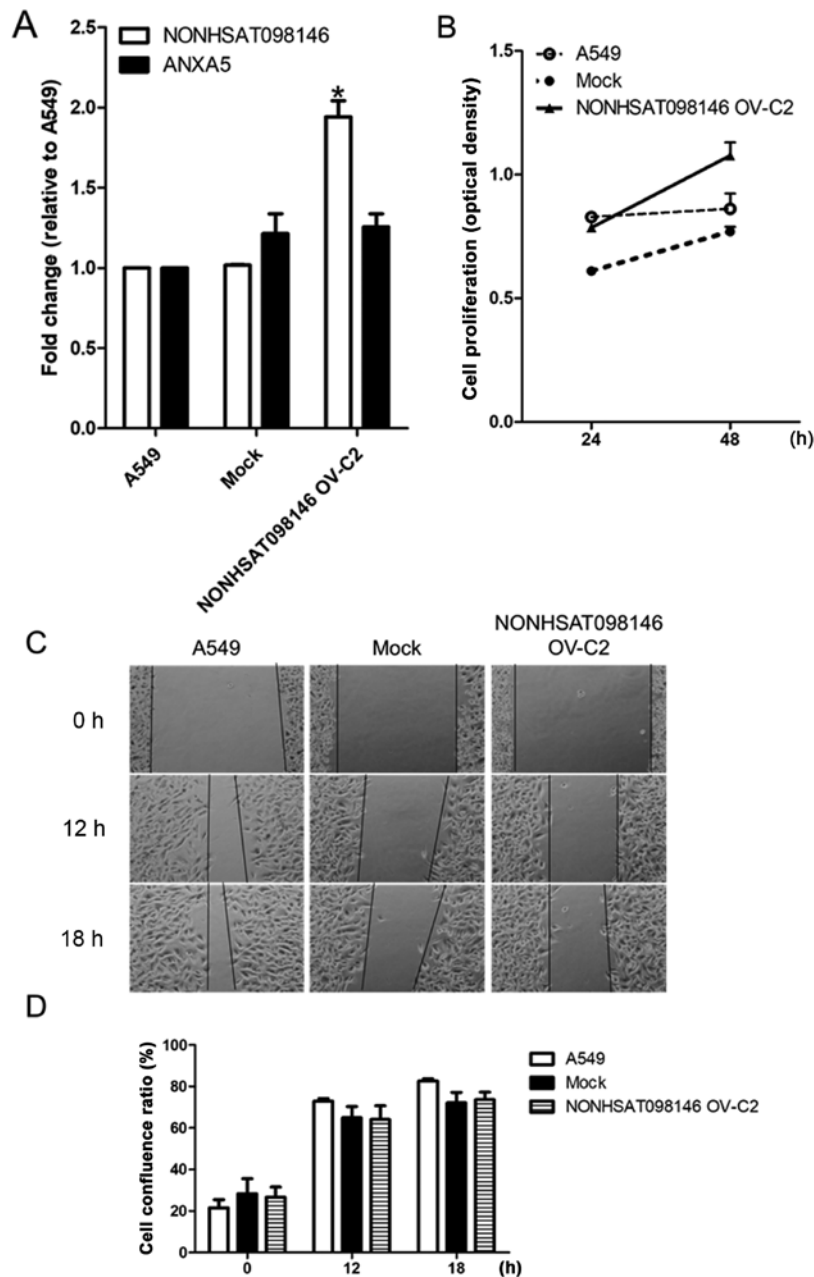
Figure 10. Established NONHSAT098146-overexpressing stable clone. (A) Total RNA was isolated and subjected to reverse transcription-quantitative polymerase chain reaction analysis to detect the RNA expression levels of *NONHSAT098146* (white) and *ANXA5* (black) in the A549 cell line and stable clone. The fold change was standardized using mRNA expression levels of glyceraldehyde-3-phosphate dehydrogenase, relative to A549. (B) Cell proliferation was detected using the MTT assay between 24 and 48 h. The optical density of the samples was standardized using the optical density of empty wells. (C) Wound-healing assay for A549 cell line and stable clone. (D) Bar figure showing the quantitative results of the wound-healing assay. Error bars represent the standard deviation. Student's t-test was used to evaluate differences between the groups. *P<0.05, compared with the A549 group. The results are summarized from observations of three independent experiments. *ANXA5*, annexin A5; OV, overexpression.

INO80D were decreased in the A549 and mock (A549 transfected entry vector) cells transfected with siRNAs targeting *CR936609*, in accordance with the results in Fig. 5A. Only the expression levels of *CR933609* were decreased in the *CR933609*-overexpressing cells transfected with siRNAs (Fig. 11A, bottom). The overexpression of *CR933609* may counteract the inhibitory effects of siRNAs on the expression levels of *INO80D*. There were five target sites for *INO80D* knockdown, which decreased the expression of *INO80D* only; the expression of *CR933609* remained stable (Fig. 11B). The expression levels of *NONHSAT098146* and *ANXA5* were

decreased in the *NONHSAT098146*-knockdown (Fig. 12A) and in the *ANXA5*-knockdown (Fig. 12B) cells overexpressing *NONHSAT098146*. These results indicated that the lncRNA *CR933609* acts as a repressor decoy to prevent downregulation of the expression of *INO80D*, whereas *NONHSAT098146* was not a repressor decoy.

Overexpression of lncRNA CR933609 prevents downregulation of the expression levels of INO80D in endogenous miRNA-5096 treatment. As the computational results suggested that miRNA-5096 may target the *INO80D* and
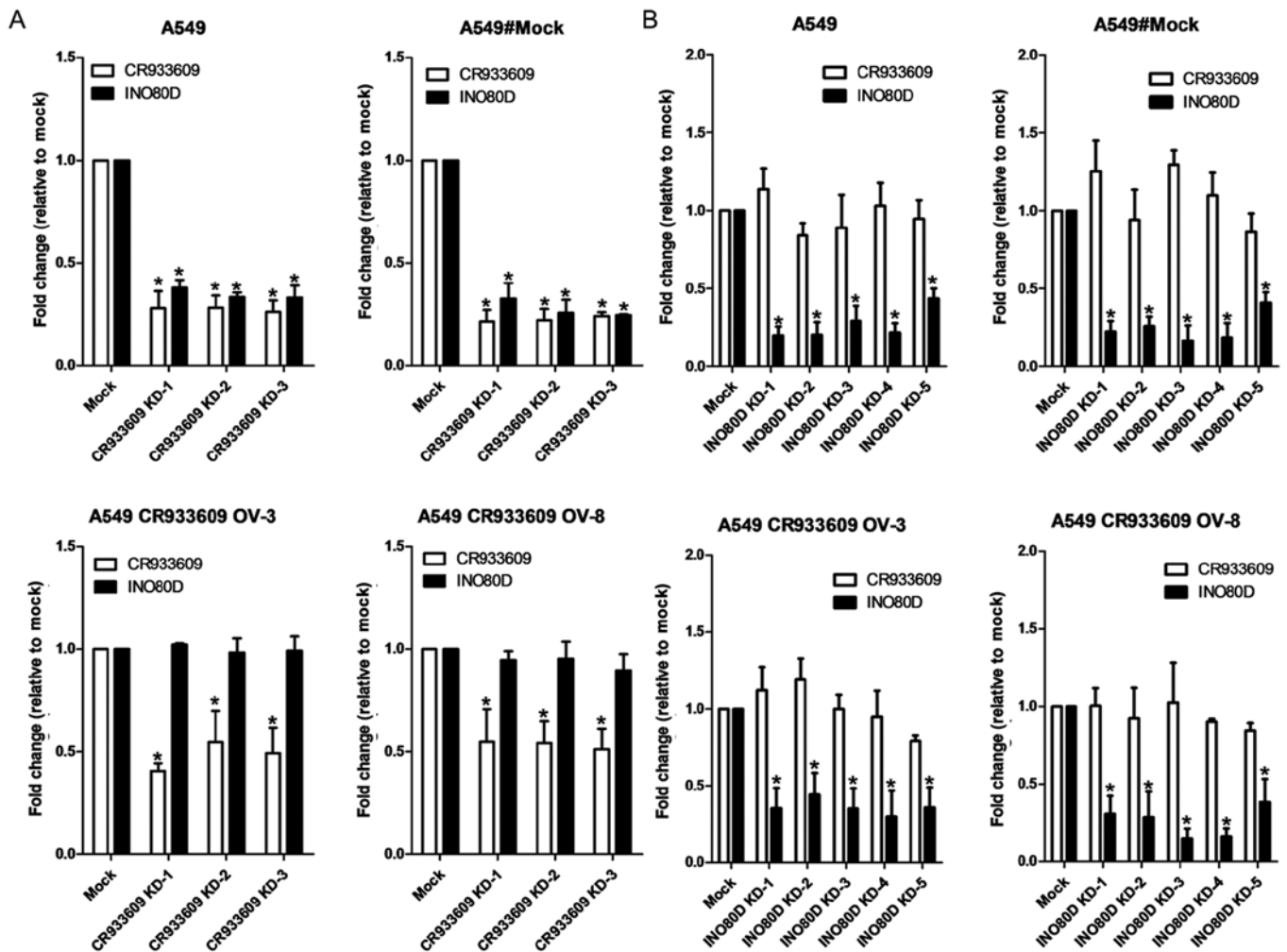
Figure 11. lncRNA *CR933609* acts as a decoy to prevent downregulation of the expression levels of *INO80D*. (A) Three target sites for *CR933609* KD were in common with those for *INO80D*. (B) Five target sites for *INO80D* KD were independent from *CR933609*. Total RNA was isolated and subjected to reverse transcription-quantitative polymerase chain reaction analysis to detect the RNA expression levels of *CR933609* (white) and *INO80D* (black) in the A549 cell line and stable clone. The fold change was standardized using mRNA expression levels of glyceraldehyde-3-phosphate dehydrogenase, relative to the mock group. Error bars represent the standard deviation. Student's t-test was used to evaluate differences between the groups. *P<0.05, compared with the mock group. The results are summarized from observations of three independent experiments. *INO80D*, INO80 complex subunit D; KD, knockdown; OV, overexpression.

CR933609 transcripts at their common sequences (Fig. 3A, bottom), the A549 and *CR933609*-overexpressing A549 cells were transfected with miRNA-5096. The results indicated that miRNA-5096 at a concentration of 100 nM downregulated the expression levels of *INO80D* and *CR933609* in the A549 cells (Fig. 13, left), but not in the *CR933609*-overexpressing A549 cells (Fig. 13, middle and right). However, miRNA-5096 at a concentration of 200 nM downregulated the expression levels of *INO80D* and *CR933609* in the A549 cells (Fig. 13, left), but decreased only the expression levels of *INO80D* in the *CR933609*-overexpressing A549 cells (Fig. 13, middle and right). Accordingly, these results suggested that *CR933609* acts as a repressor decoy to protect *INO80D* from downregulation by miRNAs.

Discussion

In the present study, a bioinformatics pipeline was constructed to identify lncRNA sequences that were similar to the 3'-UTRs of protein-coding genes, and to confirm that these lncRNA and coding gene pairs contain the same miRNA target sites. The expression levels of *CR933609* and *INO80D*, and those of *NONHSAT098146* and *ANXA5* were significantly decreased in NSCLC. In addition, the expression levels of *CR933609* and *INO80D* were significantly decreased in colon and kidney cancer, and the expression levels of *NONHSAT098146* and *ANXA5* were significantly decreased in colon, mucosal, and kidney cancer. The expression levels of *CR933609* and *INO80D* were decreased in *CR933609*-knockdown NSCLC cells, whereas only the expression levels of *INO80D* were decreased in *INO80D*-knockdown cells. The expression levels of *NONHSAT098146* and *ANXA5* were decreased in *NONHSAT098146*- and *ANXA5*-knockdown NSCLC cells. It was found that there were independent promoters in *CR933609* and *INO80D*, however, *NONHSAT098146* hybridization signals were undetectable. Furthermore, it was found that *INO80D* was downregulated by endogenous miRNA-5096 in A549 cells but not in *CR933609*-overexpressing A549 cells. Therefore, the lncRNA *CR933609* may act as a decoy to protect *INO80D* from downregulation by miRNA-5096
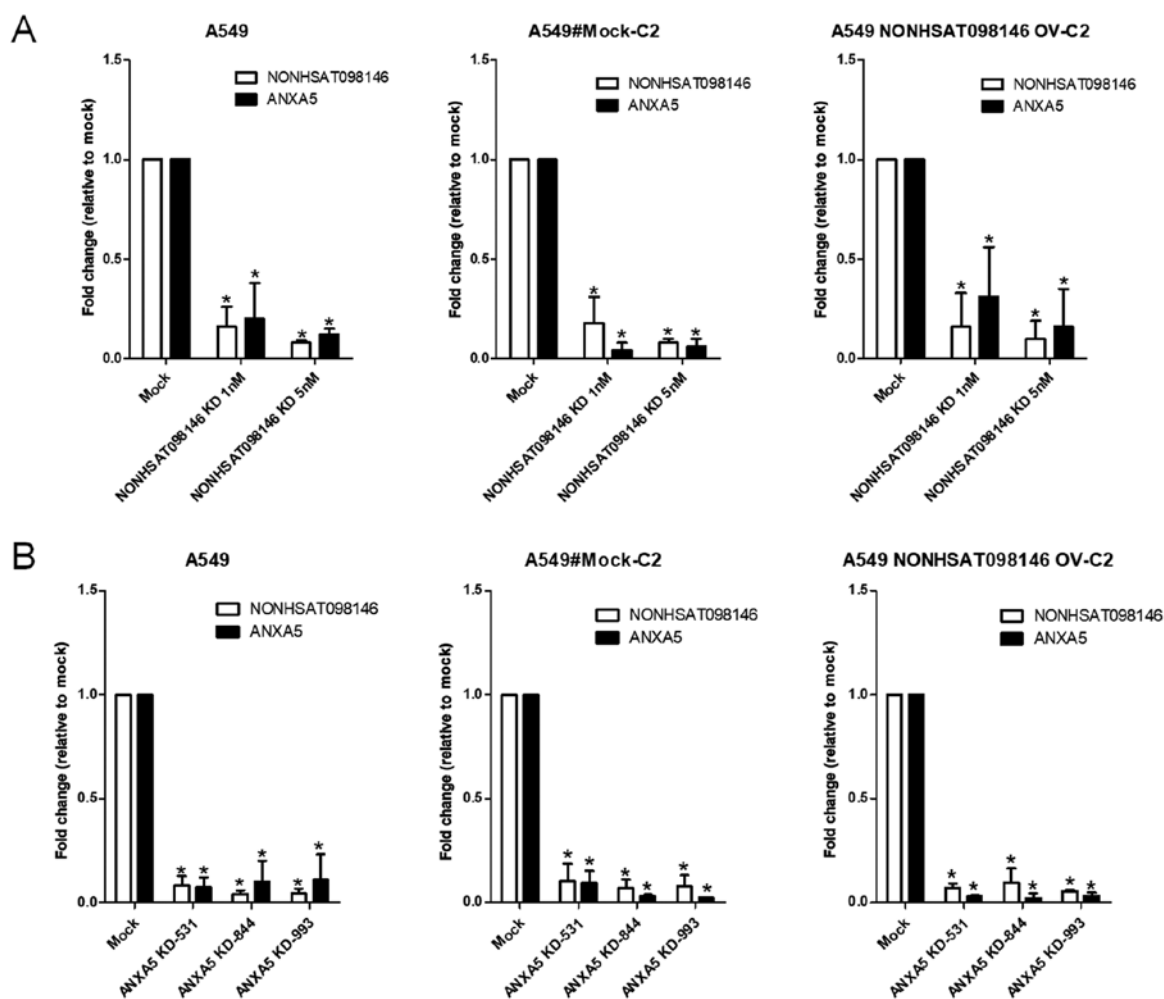
Figure 12. Expression levels of *NONHSAT098146* and *ANXA5* do not between *A549* and *NONHSAT098146*-overexpressing stable cell lines. (A) One target site for *NONHSAT098146* KD (1 and 5 nM) was in common with those for *ANXA5*. (B) Three target sites for *ANXA5* KD were independent from *NONHSAT098146*. Total RNA was isolated and subjected to reverse transcription-quantitative polymerase chain reaction analysis to detect RNA expression levels of *NONHSAT098146* (white) and *ANXA5* (black) in the A549 cell line and stable clone. The fold change was standardized using mRNA expression levels of glyceraldehyde-3-phosphate dehydrogenase, relative to the mock group. Error bars represent the standard deviation. Student's t-test was used to evaluate differences between the groups. *P<0.05, compared with the mock group. The results are summarized from observations of three independent experiments. *ANXA5*, annexin A5; KD, knockdown; OV, overexpression.
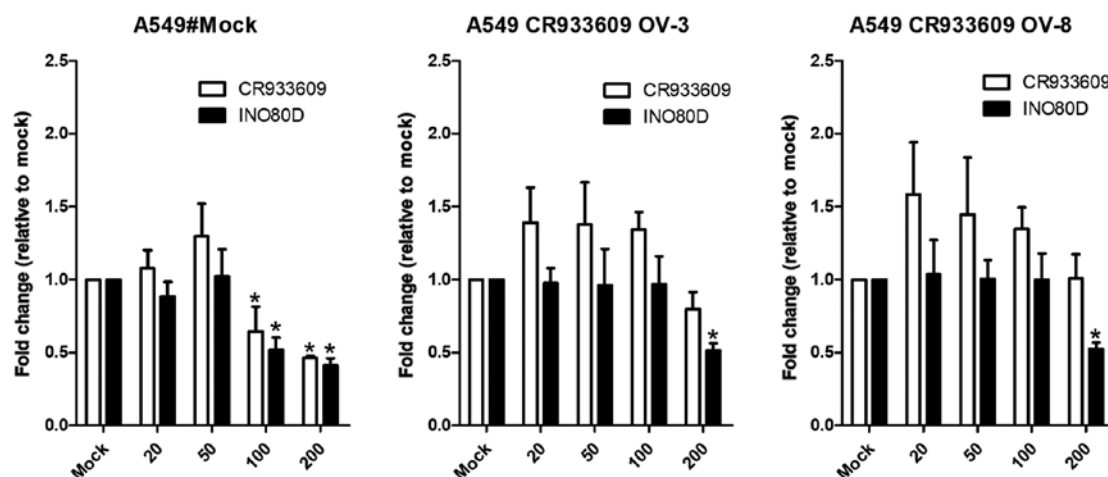

Figure 13. Overexpression of *CR933609* prevents downregulation of expression levels of *INO80D* in endogenous miRNA-5096 treatment. miRNA-5096 was transfected into the A549 stable clone. The dose of miRNA was 20-200 nM. Total RNA was isolated and subjected to reverse transcription-quantitative polymerase chain reaction analysis to detect RNA expression levels of *CR933609* (white) and *INO80D* (black) in the A549 stable clone. The fold change was standardized using mRNA expression levels of *GAPDH* and expressed relative to the mock group. Error bars represent the standard deviation. Student's t-test was used to evaluate differences between the groups. *P<0.05, compared with the mock group. The results were summarized from observations of three independent experiments. miRNA, microRNA; *INO80D*, INO80 complex subunit D; OV, overexpression.

in NSCLC cells. Thus, a protocol was established to identify novel lncRNAs in 3'-UTRs.

The interaction of RNA-binding proteins and miRNAs with the 3'-UTRs of mRNAs is known to affect the expression of eukaryotic genes by regulating mRNA translation, stability, and subcellular localization (44,45). The present study tested the hypothesis that, in addition to miRNAs, lncRNAs are involved in posttranscriptional gene regulation. A genome-wide computational pipeline identified 12 human lncRNA transcripts that showed high sequence matches with the 3'-UTRs of protein-coding mRNAs, suggesting that lncRNAs may be miRNA decoys (Fig. 1B and C). The protein-coding genes matching this set of 12 lncRNAs were involved in regulation of translational initiation and receptor binding, and their promoters contained similar transcription factor binding sites. Two of these lncRNA/coding-gene pairs, *CR933609* and *INO80D*, and *NONHSAT098146* and *ANXA5* were investigated. Notably, the transcription unit of the lncRNA *CR933609* was found to be embedded within the 3'-UTR of the *INO80D* gene (Fig. 3A), whereas *CR933609* had a distinct promoter region (Fig. 6). Furthermore, the lncRNA *NONHSAT098146* was identified as an artificial gene (Figs. 7 and 8). The results indicated that certain lncRNAs embedded in coding genes may not be transcripts, and a distinct promoter region requires identification.

To examine the biological functions of *CR933609* and *INO80D*, RNA interference experiments were performed using artificial siRNAs (targeting sequences common to both transcripts) and shRNAs (specific for *INO80D*). The lncRNA *CR933609* was expressed at significantly lower levels in three types of tumor tissue, compared with adjacent normal tissues (Fig. 4A). In addition, cell migration decreased in A549 clonal lines overexpressing *CR933609* (Fig. 9). Therefore, *CR933609* may act as a tumor suppressor gene in A549 cells. Notably, the expression levels of *INO80D* were downregulated in the *CR933609*- and *INO80D*-knockdown cells, whereas the lncRNA *CR933609* was downregulated in *CR933609*-knockdown NSCLC cells (Fig. 5A). However, no significant changes were observed in the expression level of *INO80D* following *CR933609* knockdown in *CR933609*-overexpressing cells (Fig. 11A). Additionally, endogenous miRNA-5096 downregulated *CR933609* and *INO80D* in A549 cells, but a different pattern was observed in *CR933609*-overexpressing A549 cells (Fig. 13). Previous data have shown that the expression level of miRNA-5096 was reduced, whereas the expression level of miRNA-4694-3p was not altered significantly in lung cancer (46). *CR933609* acted as a decoy to prevent the downregulation of *INO80D*.

Chromatin remodeling is the dynamic modification of chromatin architecture to allow condensed genomic DNA access to the regulatory transcription machinery, thereby controlling gene expression (47). It also provides fine-tuning at crucial cell growth and division steps to suppress tumor development. Targeting of the chromatin remodeling pathways is currently emerging as a major therapeutic strategy for the treatment of several types of cancer. *INO80D* encodes subunit D of the INO80 chromatin remodeling complex and is involved in transcriptional regulation, DNA replication and DNA repair, and may also be crucial in tumorigenesis (48). The data in the present study suggested that the lncRNA *CR933609* regulated

the mRNA stability of *INO80D* by competing for transcriptional enhancers or repressors. Therefore, the lncRNA *CR933609* is likely to be involved in chromatin remodeling through the regulation of *INO80D*. Furthermore, the present study found that the lncRNA *CR933609* may act as a tumor suppressor by regulating NSCLC cell migration (Fig. 9), and may serve as a repressor decoy to prevent the downregulation of *INO80D* (Fig. 11). Chromatin remodeling is one of the most important mechanisms for DNA repair, particularly in DNA DSBs. DNA DSBs result in cell cycle checkpoint arrest and apoptosis. This response can suspend tumorigenesis. The appropriate regulation of the mechanisms involved in DNA DSBs, including chromatin remodeling, is critical (49). Therefore, the lncRNA *CR933609*, which acts as a decoy to protect *INO80D*, a chromatin remodeling regulator, is essential for cell survival.

3'-UTRs can be independently expressed as developmentally regulated lncRNAs, which further blurs the distinction between coding and non-coding RNAs (50). This serves as a reminder that the traditional concept of the gene is becoming increasingly outmoded (51,52). However, compared with coding RNA and miRNA, significant gaps in the understanding of lncRNA function remain. To examine whether other lncRNAs, which may likewise be embedded within protein-coding genes, also function as repressor decoys, similar experiments on the remaining 11 lncRNA/coding-gene pairs examined in *in silico* analyses can be performed. When the NONCODE database updated to the second edition, NONHSAT143029 and NONHSAT055977 had been removed from the database (30). This indicated that the novel lncRNA from the database required confirmation. The present study established a protocol to identify novel lncRNAs in the 3'-UTR and confirmed the existence of novel lncRNAs using promoter activity or northern blotting.

As there are defects in all of the bioinformatics analytical methods, a protocol was established in the present study to verify the results of the analysis. It was also found that the lncRNAs published in databases may not exist. It is necessary to detect the existence of an lncRNA prior to investigating its function. This may be the reason that certain lncRNAs were removed from the database a number of years following publication.

In conclusion, the present first constructed a bioinformatics pipeline to investigate genome-wide 3'-UTR lncRNAs and then identified their clinical significance. The results indicated that the lncRNA *CR933609* may act as a repressor decoy to protect INO80D from downregulation in NSCLC.

nos. DMR-107-206, ASIA104-CMUH-22 and ASIA105-CMUH-15).

Availability of data and materials

The datasets used and/or analyzed during the current study are available from the corresponding author on reasonable request.

Authors' contributions

CCC, TYL, YTL, YSC, YLC, YCC, CCL and PCL detected the biological function of cells, performed the RT-qPCR assays, performed the cell proliferation and luciferase reporter assays, performed the statistical analysis, and assisted in drafting the manuscript. WLC conceived the study, participated in the bioinformatics analysis, and coordinated and drafted the manuscript. KTY provided the tissue samples and the clinical data. YSC, WLC, JGC and TCL conceived the study, participated in its design and coordination, and assisted in drafting the manuscript. All authors read and approved the final manuscript.

Ethics approval and consent to participate

All participants provided their written informed consent to participate in the present study. The institutional review boards of CMUH and CCH approved the study (CMUH102-RECJ-015 and CCH-IRB-080322) and the consent procedure.

Consent for publication

All participants provided their written informed consent to participate in the present study. The publication of such data does not compromise anonymity.

Competing interests

The authors declare that they have no competing interests.

References

1. Esteller M: Non-coding RNAs in human disease. Nat Rev Genet 12: 861-874, 2011.
2. Filipowicz W, Bhattacharyya SN and Sonenberg N: Mechanisms of post-transcriptional regulation by microRNAs: Are the answers in sight? Nat Rev Genet 9: 102-114, 2008.
3. Ilott NE and Ponting CP: Predicting long non-coding RNAs using RNA sequencing. Methods 63: 50-59, 2013.
4. Wilusz JE, Sunwoo H and Spector DL: Long noncoding RNAs: Functional surprises from the RNA world. Genes Dev 23: 1494-1504, 2009.
5. Mercer TR, Dinger ME and Mattick JS: Long non-coding RNAs: Insights into functions. Nat Rev Genet 10: 155-159, 2009.
6. Kung JT, Colognori D and Lee JT: Long noncoding RNAs: Past, present, and future. Genetics 193: 651-669, 2013.
7. Hung T and Chang HY: Long noncoding RNA in genome regulation: Prospects and mechanisms. RNA Biol 7: 582-585, 2010.
8. He Y, Meng XM, Huang C, Wu BM, Zhang L, Lv XW and Li J: Long noncoding RNAs: Novel insights into hepatocelluar carcinoma. Cancer Lett 344: 20-27, 2014.
9. Tsai MC, Manor O, Wan Y, Mosammaparast N, Wang JK, Lan F, Shi Y, Segal E and Chang HY: Long noncoding RNA as modular scaffold of histone modification complexes. Science 329: 689-693, 2010.
10. Chen W, Böcker W, Brosius J and Tiedge H: Expression of neural BC200 RNA in human tumours. J Pathol 183: 345-351, 1997.
11. Iacoangeli A, Lin Y, Morley EJ, Muslimov IA, Bianchi R, Reilly J, Weedon J, Diallo R, Böcker W and Tiedge H: BC200 RNA in invasive and preinvasive breast cancer. Carcinogenesis 25: 2125-2133, 2004.
12. Berteaux N, Lottin S, Adriaenssens E, Van Coppenolle F, Leroy X, Coll J, Dugimont T and Curgy JJ: Hormonal regulation of H19 gene expression in prostate epithelial cells. J Endocrinol 183: 69-78, 2004.
13. Brannan CI, Dees EC, Ingram RS and Tilghman SM: The product of the H19 gene may function as an RNA. Mol Cell Biol 10: 28-36, 1990.
14. Gabory A, Jammes H and Dandolo L: The H19 locus: Role of an imprinted non-coding RNA in growth and development. BioEssays 32: 473-480, 2010.
15. Hibi K, Nakamura H, Hirai A, Fujikake Y, Kasai Y, Akiyama S, Ito K and Takagi H: Loss of H19 imprinting in esophageal cancer. Cancer Res 56: 480-482, 1996.
16. Zhou W, Ye XL, Xu J, Cao MG, Fang ZY, Li LY, Guan GH, Liu Q, Qian YH and Xie D: The lncRNA H19 mediates breast cancer cell plasticity during EMT and MET plasticity by differentially sponging miR-200b/c and let-7b. Sci Signal 10: 10, 2017.
17. Guo F, Li Y, Liu Y, Wang J, Li Y and Li G: Inhibition of metastasis-associated lung adenocarcinoma transcript 1 in CaSki human cervical cancer cells suppresses cell proliferation and invasion. Acta Biochim Biophys Sin (Shanghai) 42: 224-229, 2010.
18. Ji P, Diederichs S, Wang W, Böing S, Metzger R, Schneider PM, Tidow N, Brandt B, Buerger H, Bulk E, *et al*: MALAT-1, a novel noncoding RNA, and thymosin beta4 predict metastasis and survival in early-stage non-small cell lung cancer. Oncogene 22: 8031-8041, 2003.
19. Lin R, Maeda S, Liu C, Karin M and Edgington TS: A large noncoding RNA is a marker for murine hepatocellular carcinomas and a spectrum of human carcinomas. Oncogene 26: 851-858, 2007.
20. Krüger J and Rehmsmeier M: RNAhybrid: microRNA target prediction easy, fast and flexible. Nucleic Acids Res 34 (Web Server): W451-4, 2006.
21. Wang XS, Zhang Z, Wang HC, Cai JL, Xu QW, Li MQ, Chen YC, Qian XP, Lu TJ, Yu LZ, *et al*: Rapid identification of UCA1 as a very sensitive and specific unique marker for human bladder carcinoma. Clin Cancer Res 12: 4851-4858, 2006.
22. Zuo ZK, Gong Y, Chen XH, Ye F, Yin ZM, Gong QN and Huang JS: TGFβ1-induced lncRNA UCA1 upregulation promotes gastric cancer invasion and migration. DNA Cell Biol 36: 159-167, 2017.
23. Wang Y, Zhang H, Li X and Chen W: Differential expression profile analysis of lncRNA UCA1α regulated mRNAs in bladder cancer. J Cell Biochem 119: 1841-1854, 2018.
24. Nakagawa T, Endo H, Yokoyama M, Abe J, Tamai K, Tanaka N, Sato I, Takahashi S, Kondo T and Satoh K: Large noncoding RNA HOTAIR enhances aggressive biological behavior and is associated with short disease-free survival in human non-small cell lung cancer. Biochem Biophys Res Commun 436: 319-324, 2013.
25. Ülger Y, Dadaş E, Yalinbaş Kaya B, Sümbül AT, Genç A and Bayram S: The analysis of lncRNA HOTAIR rs12826786 C>T polymorphism and gastric cancer susceptibility in a Turkish population: Lack of any association in a hospital-based case-control study. Ir J Med Sci 186: 859-865, 2017.
26. Wu X, Cao X and Chen F: LncRNA-HOTAIR activates tumor cell proliferation and migration by suppressing miR-326 in cervical cancer. Oncol Res: Aug 31, 2017 (Epub ahead of print). doi: 10.3727/096504017X15037515496840.
27. Han L, Kong R, Yin DD, Zhang EB, Xu TP, De W and Shu YQ: Low expression of long noncoding RNA GAS6-AS1 predicts a poor prognosis in patients with NSCLC. Med Oncol 30: 694, 2013.
28. Poliseno L, Salmena L, Zhang J, Carver B, Haveman WJ and Pandolfi PP: A coding-independent function of gene and pseudogene mRNAs regulates tumour biology. Nature 465: 1033-1038, 2010.
29. Chan WL, Yuo CY, Yang WK, Hung SY, Chang YS, Chiu CC, Yeh KT, Huang HD and Chang JG: Transcribed pseudogene ψPPM1K generates endogenous siRNA to suppress oncogenic cell growth in hepatocellular carcinoma. Nucleic Acids Res 41: 3734-3747, 2013.
30. Bu D, Yu K, Sun S, Xie C, Skogerbø G, Miao R, Xiao H, Liao Q, Luo H, Zhao G, *et al*: NONCODE v3.0: Integrative annotation of long noncoding RNAs. Nucleic Acids Res 40D: D210-D215, 2012.

31. Kozomara A and Griffiths-Jones S: miRBase: Integrating microRNA annotation and deep-sequencing data. Nucleic Acids Res 39 (Database): D152-D157, 2011.
32. Karolchik D, Barber GP, Casper J, Clawson H, Cline MS, Diekhans M, Dreszer TR, Fujita PA, Guruvadoo L, Haeussler M, et al: The UCSC Genome Browser database: 2014 update. Nucleic Acids Res 42D: D764-D770, 2014.
33. Hsu SD, Lin FM, Wu WY, Liang C, Huang WC, Chan WL, Tsai WT, Chen GZ, Lee CJ, Chiu CM, et al: miRTarBase: A database curates experimentally validated microRNA-target interactions. Nucleic Acids Res 39 (Suppl. 1): D163-D169, 2011.
34. Hsu SD, Tseng YT, Shrestha S, Lin YL, Khaleel A, Chou CH, Chu CF, Huang HY, Lin CM, Ho SY, et al: miRTarBase update 2014: An information resource for experimentally validated miRNA-target interactions. Nucleic Acids Res 42D: D78-D85, 2014.
35. Friedman RC, Farh KK, Burge CB and Bartel DP: Most mammalian mRNAs are conserved targets of microRNAs. Genome Res 19: 92-105, 2009.
36. Grimson A, Farh KK, Johnston WK, Garrett-Engele P, Lim LP and Bartel DP: MicroRNA targeting specificity in mammals: Determinants beyond seed pairing. Mol Cell 27: 91-105, 2007.
37. Lewis BP, Burge CB and Bartel DP: Conserved seed pairing, often flanked by adenosines, indicates that thousands of human genes are microRNA targets. Cell 120: 15-20, 2005.
38. John B, Enright AJ, Aravin A, Tuschl T, Sander C and Marks DS: Human microRNA targets. PLoS Biol 2: e363, 2004.
39. Livak KJ and Schmittgen TD: Analysis of relative gene expression data using real-time quantitative PCR and the 2(-Δ Δ C(T)) Method. Methods 25: 402-408, 2001.
40. Sherman BT, Huang da W, Tan Q, et al: Sherman BT, Huang W, Tan Q, Guo Y, Bour S, Liu D, Stephens R, Baseler MW, Lane HC and Lempicki RA: DAVID Knowledgebase: A gene-centered database integrating heterogeneous gene annotation resources to facilitate high-throughput gene functional analysis. BMC Bioinformatics 8: 426, 2007.
41. Jeggo PA and Downs JA: Roles of chromatin remodellers in DNA double strand break repair. Exp Cell Res 329: 69-77, 2014.
42. Andrews NW, Corrotte M and Castro-Gomes T: Above the fray: Surface remodeling by secreted lysosomal enzymes leads to endocytosis-mediated plasma membrane repair. Semin Cell Dev Biol 45: 10-17, 2015.
43. Jemal A, Bray F, Center MM, Ferlay J, Ward E and Forman D: Global cancer statistics. CA Cancer J Clin 61: 69-90, 2011.
44. Kuersten S and Goodwin EB: The power of the 3' UTR: Translational control and development. Nat Rev Genet 4: 626-637, 2003.
45. Seiler J, Breinig M, Caudron-Herger M, Polycarpou-Schwarz M, Boutros M and Diederichs S: The lncRNA VELUCT strongly regulates viability of lung cancer cells despite its extremely low abundance. Nucleic Acids Res 45: 5458-5469, 2017.
46. Xie L, Yang Z, Li G, Shen L, Xiang X, Liu X, Xu D, Xu L, Chen Y, Tian Z, et al: Genome-wide identification of bone metastasis-related microRNAs in lung adenocarcinoma by high-throughput sequencing. PLoS One 8: e61212, 2013.
47. Chen T and Dent SY: Chromatin modifiers and remodellers: Regulators of cellular differentiation. Nat Rev Genet 15: 93-106, 2014.
48. Ho L and Crabtree GR: Chromatin remodelling during development. Nature 463: 474-484, 2010.
49. Delia D and Mizutani S: The DNA damage response pathway in normal hematopoiesis and malignancies. Int J Hematol 106: 328-334, 2017.
50. Dinger ME, Pang KC, Mercer TR and Mattick JS: Differentiating protein-coding and noncoding RNA: Challenges and ambiguities. PLOS Comput Biol 4: e1000176, 2008.
51. Dinger ME, Amaral PP, Mercer TR and Mattick JS: Pervasive transcription of the eukaryotic genome: Functional indices and conceptual implications. Brief Funct Genomics Proteomics 8: 407-423, 2009.
52. Gerstein MB, Bruce C, Rozowsky JS, Zheng D, Du J, Korbel JO, Emanuelsson O, Zhang ZD, Weissman S and Snyder M: What is a gene, post-ENCODE? History and updated definition. Genome Res 17: 669-681, 2007.